




Article – Gregory Yu. Ivanyuk memorial issue

Trigonal variation in the garnet supergroup: the crystal structure of nikhmelnikovite, $\text{Ca}_{12}\text{Fe}^{2+}\text{Fe}_3^{3+}\text{Al}_3(\text{SiO}_4)_6(\text{OH})_{20}$, from Kovdor massif, Kola Peninsula, Russia

Sergey V. Krivovichev^{1,2*} , Taras L. Panikorovskii^{1,2}, Victor N. Yakovenchuk¹, Ekaterina A. Selivanova¹ and Gregory Yu. Ivanyuk^{1†}

¹Kola Science Centre, Russian Academy of Sciences, 14 Fersman Street, Apatity 184200, Russia; and ²Department of Crystallography, St. Petersburg State University, 7/9 University Emb., St. Petersburg, 199034, Russia

Abstract

The crystal structure of nikhmelnikovite, $\text{Ca}_{12}\text{Fe}^{2+}\text{Fe}_3^{3+}\text{Al}_3(\text{SiO}_4)_6(\text{OH})_{20}$, a new member of the garnet supergroup from Kovdor massif, Kola Peninsula, Russia ($R\bar{3}$, $a = 17.2072(6)$, $c = 10.5689(4)$ Å, $V = 2710.1(2)$ Å³ and $Z = 3$) has been refined to $R_1 = 0.046$ on the basis of 1184 unique observed reflections. Nikhmelnikovite is the first mineral species in the garnet supergroup that has a trigonal (rhombohedral) symmetry. The relationship between its unit cell and the pseudocubic (ideal garnet) unit cell can be described by the transformation matrix $[1\bar{1}0 \mid 01\bar{1} \mid \frac{1}{2}\frac{1}{2}\frac{1}{2}]$. The crystal-chemical relations between the ideal $Ia\bar{3}d$ garnet and the nikhmelnikovite structure type can be described by the following series of imaginary modifications: (1) the symmetry is lowered according to the $Ia\bar{3}d \rightarrow R\bar{3}$ group-subgroup relationship; (2) the cation sites are split according to the following sequences: $X \rightarrow \{X1, X2\}$; $Y \rightarrow \{Y1, Y2, Y3, Y4\}$; $Z \rightarrow \{Z1, Z2\}$; (3) the X sites remain fully occupied by Ca; (4) each Y site is occupied predominantly by a distinct chemical species: $Y1 \rightarrow \text{Al}$ (Al site), $Y2 \rightarrow \text{Fe}^{2+}$ (Fe1 site), $Y3 \rightarrow \text{Fe}^{3+}$ (Fe2 site), $Y4 \rightarrow$ vacancy (Mn site); (5) one of the Z sites ($Z1$) is occupied by Si, whereas the other site ($Z2$) is predominantly vacant. The crystal-chemical formula that takes into account the transition between the archetype and the nikhmelnikovite structure type can be described as $^X\{\text{Ca}_{12}\}^Y[\text{Fe}^{2+}\text{Al}_4\text{Fe}_3^{3+}\square]^Z(\text{Si}_6\square_6)\text{O}_{24}(\text{OH})_{20}\square_4$. The structural complexity of nikhmelnikovite (4.529 bit/atom and 434.431 bit/cell, after H-correction) is higher than those for andradite, grossular and katoite, which is typical for low-temperature minerals formed after primary minerals with simpler structures.

Keywords: garnet, nikhmelnikovite, crystal structure, Kovdor, Kola peninsula, Russian Arctic

(Received 20 January 2021; accepted 24 June 2021; Accepted Manuscript published online: 28 June 2021; Associate Editor: Juraj Majzlan)

Introduction

Minerals of the garnet supergroup are common rock-forming and accessory minerals of different metamorphic and metasomatic rocks, including skarns and skarn-like rocks associated with carbonatites in alkaline-ultrabasic complexes. In particular, Ti-rich andradite is a common mineral of skarn-like rocks of the Kovdor massif, Kola Peninsula, Russia (Ivanyuk *et al.*, 2002), where it forms well shaped rhombic dodecahedral crystals (up to 3 cm in diameter), spherical porphyroblasts (up to 5 cm in diameter) and coarse-grained monomineralic segregations (up to 20 cm in diameter).

The late stage of skarn formation may include low-temperature crystallisation of secondary garnet-group mineral phases with the ‘hydrogarnet-type’ substitution according to the scheme $4\text{H}^+ + \text{Z}\square \rightarrow \square + \text{Z}\text{Si}^{4+}$ (Lager *et al.*, 1989; Grew *et al.*, 2013). Such a phase was indeed found as thin crusts covering andradite crystals at Kovdor. Its detailed study led to its recognition as a new

mineral species, nikhmelnikovite, $\text{Ca}_{12}\text{Fe}^{2+}\text{Fe}_3^{3+}\text{Al}_3(\text{SiO}_4)_6(\text{OH})_{20}$, which, in contrast to all known garnet-supergroup minerals, has a trigonal symmetry (Krivovichev *et al.*, 2019). In the present contribution, we provide the results of its crystal-structure determination and describe its relationship to other minerals of the garnet supergroup. It is remarkable that nikhmelnikovite was found in association with manaevite-(Ce), the first H_2O -bearing member of the vesuvianite group, which also formed by the substitution of $(\text{SiO}_4)^{4-}$ groups with $[\text{H}_4\text{O}_4]^{4-}$ (Moiseev *et al.*, 2020).

Materials and methods

Background information

Nikhmelnikovite crystals studied in this work were sampled from the abandoned Mica open pit (kar’er ‘Slyuda’), also known as the Phlogopite open pit, in the Kovdor massif of ultrabasic, alkaline and carbonatitic igneous rocks and related metasomatites. The massif is situated in the southwestern part of the Murmansk Region, Russia (67°33’N, 30°31’E) (Fig. 1). The crystals were extracted from a coarse-grained spotted rock composed of white calcite, scolecite and natrolite–gonnardite (up to 5 cm in diameter), pale-blue pectolite (up to 15 cm long), colourless glagolevite (up to 3 cm in diameter), dark-brown andradite

*Author for correspondence: Sergey V. Krivovichev, Email: s.krivovichev@ksc.ru

†Deceased

Cite this article: Krivovichev S.V., Panikorovskii T.L., Yakovenchuk V.N., Selivanova E.A. and Ivanyuk G.Y.u. (2021) Trigonal variation in the garnet supergroup: the crystal structure of nikhmelnikovite, $\text{Ca}_{12}\text{Fe}^{2+}\text{Fe}_3^{3+}\text{Al}_3(\text{SiO}_4)_6(\text{OH})_{20}$, from Kovdor massif, Kola Peninsula, Russia. *Mineralogical Magazine* 85, 620–626. <https://doi.org/10.1180/mgm.2021.55>

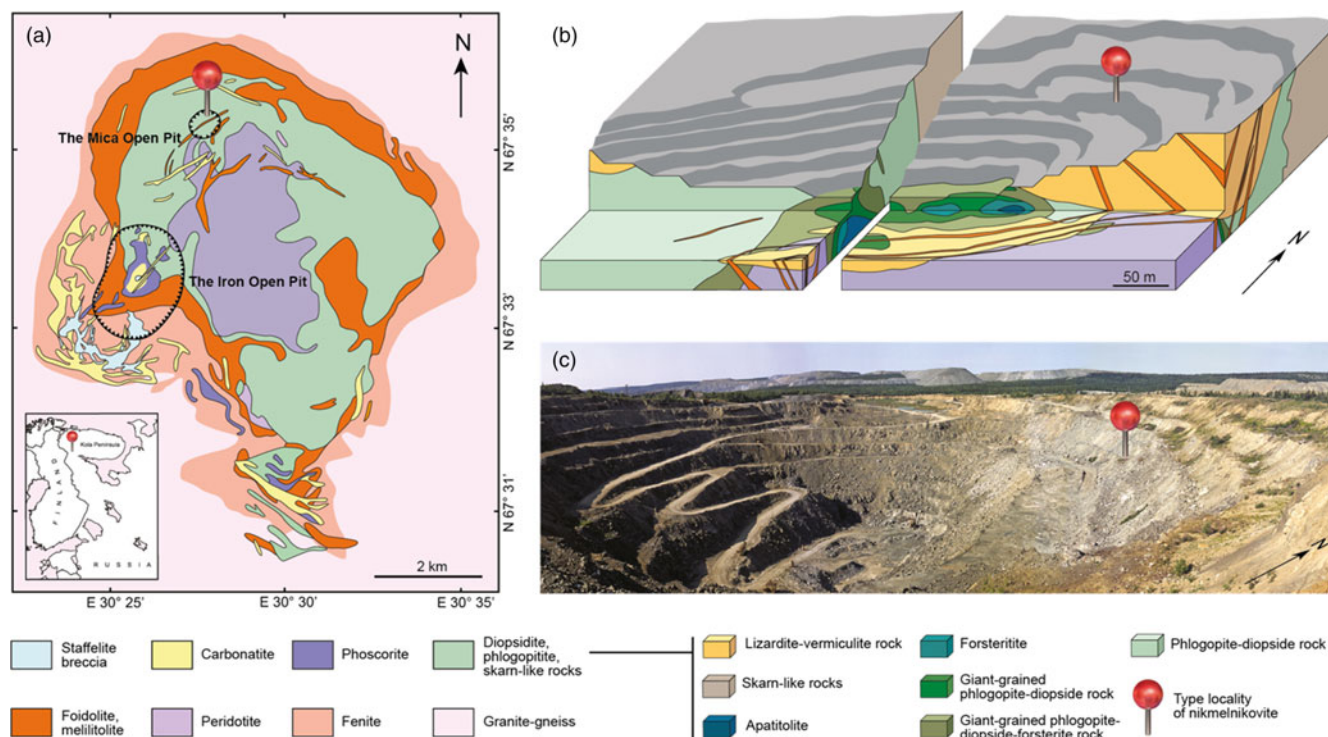


Fig. 1. Schematic geological map of the Kovdor massif (after Mikhailova *et al.*, 2016), block-diagram of the Kovdor Phlogopite Deposit (after N.M. Manaev, unpublished map) and a photo of the Mica open pit (after Ivanyuk *et al.*, 2002), indicating the nikhelnikovite type locality.

(up to 6 cm in diameter) with relict grains of magnetite, bright-green to dark-brown vesuvianite (up to 4 cm in diameter) and black magnesio-hastingsite (up to 1.5 cm long). Nikhelnikovite forms thin (up to 1 mm thick) epitaxial coatings on the octahedral faces of andradite crystals included in cavernous calcite (Fig. 2a,b,c). These crusts are in turn encrusted by crystals (up to 100 μm in diameter, Fig. 2d,e) and spherical globules (up to 5 μm in diameter, Fig. 2d) of H_4O_4 -substituted mineral of the andradite-grossular series. In back-scattered electron images, the examined crystals of andradite comprise a sector-zoned core, where variations in average atomic number reflect different Al/Fe ratios, and a thin (up to 10 μm thick) marginal zone composed of an inner Fe-rich and outer Al-rich layers. Merohedral twinning with a twofold axis oriented parallel to [110] was observed (see below).

The chemical composition of the mineral corresponds to the empirical formula $\text{Ca}_{11.81}(\text{Fe}_{0.74}^{2+}\text{Mn}_{0.12}\text{Mg}_{0.16})_{\Sigma 1.02}(\text{Al}_{3.95}\text{Fe}_{1.98}^{3+})_{\Sigma 5.93}[\text{Si}_{6.14}\text{O}_{24}](\text{OH})_{20}\cdot 1.18\text{H}_2\text{O}$ (Krivovichev *et al.*, 2019); its idealised formula can be written as $\text{Ca}_{12}\text{Fe}^{2+}\text{Al}_4\text{Fe}_2^{3+}[\text{SiO}_4]_6(\text{OH})_{20}$.

Single-crystal X-ray diffraction

The single-crystal X-ray diffraction study of nikhelnikovite was done using an Agilent Technologies Xcalibur Eos diffractometer equipped with a CCD area detector and operated at 50 kV and 40 mA. A hemisphere of three-dimensional data was collected at room temperature using monochromatic $\text{MoK}\alpha$ X-radiation ($\lambda = 0.71069 \text{ \AA}$) with frame widths of 1° and 150 s count for each frame. The intensity data were reduced and corrected for Lorentz, polarisation and background effects. Empirical absorption correction was applied in the *CrysAlisPro* (Agilent Technologies, 2014) program complex using spherical harmonics,

implemented in the *SCALE3 ABSPACK* scaling algorithm. The crystal structure was solved by direct methods with the *ShelX* program package (Sheldrick, 2008) and refined to $R_1 = 0.046$ for 1184 independent reflections with $F_o > 4\sigma(F_o)$. Crystal data, data collection information and structure refinement details are given in Table 1, final atom positions, displacement parameters and site occupancies are listed in Table 2. Selected interatomic distances are reported in Table 3. The crystal structure of nikhelnikovite was solved in the space group $R\bar{3}$ using a merohedral twin model (2-fold axis along [110]) with a twin ratio of 0.134/0.866. The low-occupancy O9, Mn and Si2 sites were refined in an isotropic approximation, because the attempts to refine them anisotropically resulted in physically unrealistic displacement parameters. The occupancies of the O7, O9, Mn and Si2 sites were fixed in order to generate a crystal-chemically reasonable model. Anisotropic displacement parameters and other details of the crystal-structure refinement are in the crystallographic information file, which has been deposited with the Principal Editor of *Mineralogical Magazine* and is available as Supplementary material.

Results

Geometrical relationship to the ideal cubic garnet unit cell

Most of the garnet-superfamily minerals crystallise in the cubic space group $Ia\bar{3}d$. Their unit cell parameters depend upon the chemical composition; e.g. for the minerals chemically related to nikhelnikovite, grossular, $\text{Ca}_3\text{Al}_2(\text{SiO}_4)_3$, andradite, $\text{Ca}_3\text{Fe}_2(\text{SiO}_4)_3$, and katoite, $\text{Ca}_3\text{Al}_2(\text{OH})_{12}$, a is equal to 11.847, 12.063 and 12.38 \AA , respectively (Geiger and Armbruster, 1997; Armbruster and Geiger, 1993; Sacerdoti and Passaglia, 1985). Nikhelnikovite is the first mineral species in the garnet

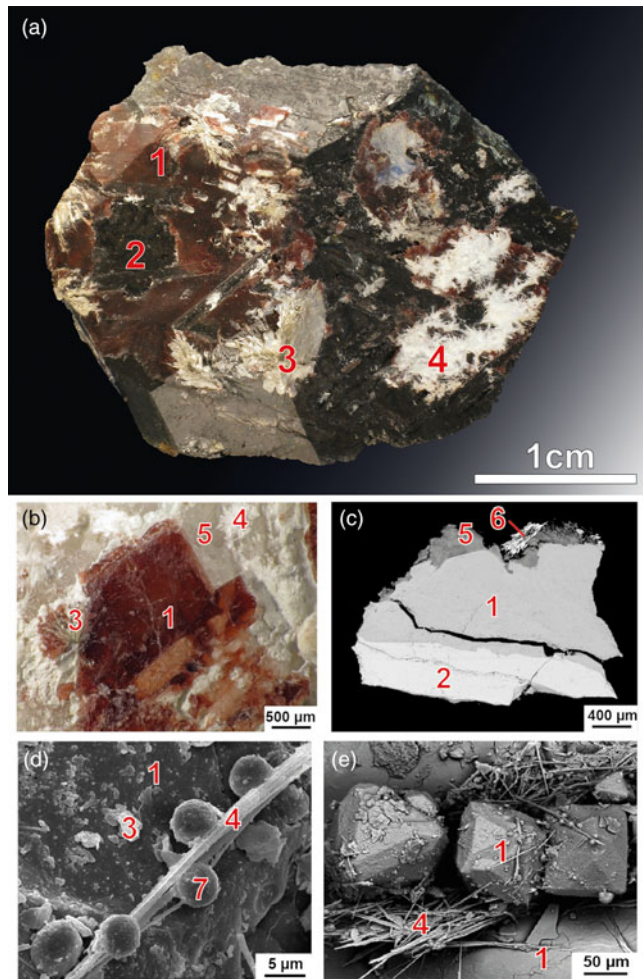


Fig. 2. Paragenesis and morphology of nikhelnikovite and associated minerals. (a,b) Crusts of nikhelnikovite (1) on andradite (2) associated with glagolevite (3), tobermorite (4) and natrolite (5). (c) Back-scattered electron image of cross-section of andradite with epitaxial nikhelnikovite crust, natrolite and later strontianite bunches (6). (d) Secondary-electron images of nikhelnikovite crust with spherulites of H_4O_2 -substituted grossular (7). (e) Octahedral aggregates of complex hydrogarnet-related phases associated with glagolevite and tobermorite.

supergroup that has a trigonal (rhombohedral) symmetry and the third IMA-recognised mineral species in the supergroup that has a non-cubic symmetry (the two others are tetragonal henritermierite and holtstamite). Nikhelnikovite crystallises in the rhombohedral space group $R\bar{3}$ with the unit cell parameters in the hexagonal setting given in Table 1. The relationship between its unit cell parameters (a_h , b_h , c_h) and those of the pseudocubic cell (a_c , b_c , c_c) are shown in Fig. 3 and can be described by the following equations:

$$a_h = a_c - b_c; b_h = b_c - c_c; c_h = \frac{1}{2}(a_c + b_c + c_c) \quad (1)$$

The corresponding transformation matrix $T_{c \rightarrow h} = [1\bar{1}0 \mid 01\bar{1} \mid \frac{1}{2}\frac{1}{2}\frac{1}{2}]$ has its determinant $\det(T) = 3/2$ that corresponds to the transition between the unit cell volumes of the real (rhombohedral in hexagonal axes) unit cell (V_h) and the pseudocubic unit cell analogous to 'common' garnet-supergroup minerals (V_{pc}). The latter value is equal to 1806.7 Å³, which is comparable to the cubic unit cell volumes of grossular, andradite and katoite (1662.7, 1755.4 and 1897.4 Å³, respectively). The pseudocubic

Table 1. Crystal data, data collection and structure refinement parameters for nikhelnikovite.

Crystal data	
Temperature (K)	293(2)
Crystal system	Trigonal
Space group	$R\bar{3}$
a (Å)	17.2072(6)
c (Å)	10.5689(4)
Volume (Å ³)	2710.1(2)
Z	3
ρ_{calc} (g/cm ³)	3.086
μ (mm ⁻¹)	3.413
$F(000)$	2518
Data collection	
Crystal size (mm)	0.23 × 0.21 × 0.12
Radiation	MoK α ($\lambda = 0.71073$)
2 θ range for data collection (°)	6.69–53.00
Index ranges	$-13 \leq h \leq 21, -19 \leq k \leq 11, -13 \leq l \leq 13$
Reflections collected	3442
Independent reflections	1184 [$R_{\text{int}} = 0.0464, R_{\text{sigma}} = 0.0487$]
Refinement	
Data/restraints/parameters	1184/0/123
Goodness-of-fit (S) on F^2	1.116
Weighting scheme	$W = 1/[S^2(F_o^2) + (0.0399P)^2 + 40.0857P]$, where $P = (F_o^2 + 2F_c^2)/3$
Final R indexes [$>4\sigma(I)$]	$R_1 = 0.046, wR_2 = 0.113$
Final R indexes [all data]	$R_1 = 0.050, wR_2 = 0.115$
$\Delta\rho_{\text{max}}, \Delta\rho_{\text{min}}$ (e ⁻ Å ⁻³)	0.75, -0.61

unit cell is a rhombohedron with the parameters $a_c = 12.180$ Å and $\alpha = 89.89^\circ$ (i.e. the rhombohedral distortion is within 0.12°).

Cation coordination and cation arrays

The idealised crystal-chemical formula of nikhelnikovite, $\text{Ca}_{12}\text{Fe}^{2+}\text{Al}_4\text{Fe}_2^{3+}[\text{SiO}_4]_6(\text{OH})_{20}$, can be rewritten as $\{\text{Ca}_{12}\}[\text{Fe}^{2+}\text{Al}_4\text{Fe}_2^{3+}](\text{Si}_6)\text{O}_{24}(\text{OH})_{20}$, in order to conform with the general formula of garnet-supergroup mineral species, $\{X_3\}[Y_2](Z_3)\varphi_{12}$, where X , Y and Z are cations in eightfold, octahedral and tetrahedral coordinations, respectively; $\varphi = \text{O}, \text{OH}$ (Grew *et al.*, 2013). In contrast to the ideal garnet structure with the space group $Ia\bar{3}d$, the nikhelnikovite structure is strongly modified through the formation of vacancies, cation ordering and substitution mechanisms. In this section, we briefly outline the modifications of cation arrays in the structure of nikhelnikovite in comparison to the ideal patterns observed in the $Ia\bar{3}d$ structure type (archetype).

The crystal structure of nikhelnikovite contains two eightfold-coordinated X sites, Ca1 and Ca2, that are fully occupied by Ca. Cation arrays in the archetype and nikhelnikovite structures are shown in Fig. 4a and b, respectively. Except for slight geometrical distortions, the Ca arrays are identical and therefore are not involved in the transition between the two structure types.

The array of octahedrally coordinated Y cations in the archetype structure (Fig. 4a) is a cubic body-centred lattice with the a_Y parameter being half that of the ideal $Ia\bar{3}d$ unit cell. There are four octahedrally coordinated cation sites in nikhelnikovite, Al, Fe1, Fe2 and Mn, all together forming the same Y -cation array as in the archetype arrangement (Fig. 4b). However, in contrast to the latter, the array is split into four distinct sites with different site occupancies. The Al site is predominantly occupied by Al with the $\langle\text{Al}-\text{O}\rangle$ bond length of 1.922 Å. The Fe1 site has the $\langle\text{Fe1}-\text{O}\rangle$ bond length equal to 2.137 Å. Its site occupancy is consistent with Fe as the major component with a small admixture of Al. The $\langle\text{Fe1}-\text{O}\rangle$ bond length corresponds to the occupation of

Table 2. Atom coordinates, displacement parameters (\AA^2) and site occupancies (s.o.f.; apfu = atoms per formula unit) in the structure of nikkelnikovite.

Site	s.o.f.	apfu	x	y	z	$U_{\text{eq}}/U_{\text{iso}}$ (\AA^2)
Al	$\text{Al}_{0.93(1)}\text{Fe}_{0.07(1)}$	$\text{Al}_{2.79}\text{Fe}_{0.21}$	$\frac{1}{2}$	$\frac{1}{2}$	0	0.0049(8)
Fe1	$\text{Fe}_{0.89(2)}\text{Al}_{0.11(2)}$	$\text{Fe}_{0.89}\text{Al}_{0.11}$	$\frac{1}{3}$	$\frac{2}{3}$	$\frac{2}{3}$	0.0070(8)
Fe2	$\text{Fe}_{0.63(1)}\text{Al}_{0.37(1)}$	$\text{Fe}_{1.89}\text{Al}_{1.11}$	$\frac{1}{2}$	$\frac{1}{2}$	$\frac{1}{2}$	0.0044(5)
Mn	$\text{Mn}_{0.118}^*$	$\text{Mn}_{0.118}$	$\frac{1}{3}$	$\frac{2}{3}$	$\frac{1}{6}$	0.004(6)
Ca1	Ca	$\text{Ca}_{6.00}$	0.63009(8)	0.62319(8)	0.75159(10)	0.0054(3)
Ca2	Ca	$\text{Ca}_{6.00}$	0.34053(9)	0.54671(8)	0.43146(10)	0.0069(3)
Si1	Si	$\text{Si}_{6.00}$	0.16156(12)	0.45334(12)	0.58313(14)	0.0063(4)
Si2	$\text{Si}_{0.118}^*$	$\text{Si}_{0.708}$	0.4998(13)	0.3757(13)	0.7459(16)	0.024(4)
O1	O	$(\text{OH})_{5.292}\text{O}_{0.708}$	0.5454(3)	0.4698(3)	0.6522(4)	0.0099(10)
O2	O	$(\text{OH})_{5.292}\text{O}_{0.708}$	0.5006(3)	0.3970(3)	0.9353(4)	0.0104(10)
O3	O	$(\text{OH})_{5.292}\text{O}_{0.708}$	0.6212(3)	0.5747(3)	0.9573(4)	0.0073(9)
O4	O	$\text{O}_{6.00}$	0.4672(3)	0.5277(3)	0.8328(4)	0.0104(10)
O5	O	$\text{O}_{6.00}$	0.5712(3)	0.6303(3)	0.5449(3)	0.0078(9)
O6	O	$\text{O}_{6.00}$	0.2359(3)	0.5590(3)	0.5535(4)	0.0070(9)
O7	$\text{O}_{0.882}^*$	$(\text{OH})_{1.764}$	$\frac{1}{3}$	$\frac{2}{3}$	0.3264(7)	0.0078(18)
O8	O	$\text{O}_{6.00}$	0.3935(3)	0.4854(3)	0.5978(4)	0.0074(9)
O9	$\text{O}_{0.118}^*$	$\text{O}_{0.708}$	0.243(4)	0.581(3)	0.279(3)	0.007(7)

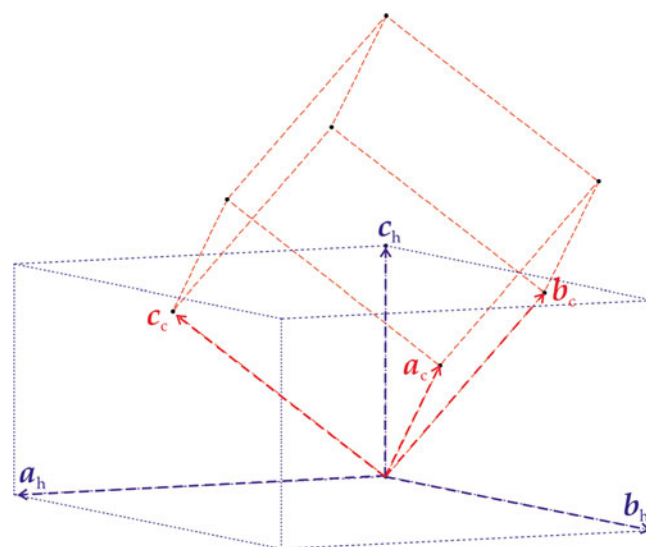
*fixed during refinement.

Table 3. Selected bond distances (\AA) in the crystal structure of nikkelnikovite.

Al–O2 ×2	1.904(4)	Ca2–O1	2.297(4)
Al–O3 ×2	1.877(4)	Ca2–O2	2.391(4)
Al–O4 ×2	1.984(4)	Ca2–O4	2.676(5)
<Al–O>	1.922	Ca2–O6	2.408(4)
		Ca2–O6	2.309(4)
Fe1–O6 ×6	2.137(4)	Ca2–O7	2.401(4)
		Ca2–O8	2.448(4)
Fe2–O1 ×2	1.968(4)	Ca2–O9	2.39(6)
Fe2–O5 ×2	2.002(4)	Ca2–O9	2.60(6)
Fe2–O8 ×2	2.008(4)	<Ca2–O>	2.434
<Fe2–O>	1.992		
		Si1–O4	1.645(5)
Mn–O9 ×6	1.93(4)	Si1–O5	1.645(5)
		Si1–O6	1.648(5)
Ca1–O1	2.519(5)	Si1–O8	1.666(4)
Ca1–O2	2.424(5)	<Si1–O>	1.651
Ca1–O3	2.384(4)		
Ca1–O3	2.306(4)	Si2–O1	1.72(2)
Ca1–O4	2.586(5)	Si2–O2	2.033(18)
Ca1–O5	2.506(4)	Si2–O3	1.89(2)
Ca1–O5	2.436(4)	Si2–O9	1.82(6)
Ca1–O8	2.411(4)	<Si2–O>	1.88
<Ca1–O>	2.447		

this site by Fe^{2+} ; this is most probably also the site that accommodates Mg^{2+} . The average <Fe2–O> bond length of 1.993 \AA and the refined site occupancy agrees well with its population by Fe^{3+} and Al. Finally, the Mn site is predominantly vacant. The assignment of Mn to this site is rather tentative, as this site may be occupied by Fe as well. The overall ratio of the octahedral sites is Al:Fe1:Fe2:Mn = 3:1:3:1, which provides eight cations in total, in agreement with the general formula of the garnet-supergroup mineral $\{X_3\}[Y_2](Z_3)\varphi_{12}$ multiplied by four, $\{X_{12}\}[Y_8](Z_{12})\varphi_{48}$.

The $Ia\bar{3}d \rightarrow R\bar{3}$ symmetry transition is associated with the splitting of the single Si site in the archetype structure into two symmetrically non-equivalent sites in the derivative, Si1 and Si2. The archetypal and derivative Si arrangements are shown in Fig. 4e and f, respectively. The Si1 site in nikkelnikovite is fully occupied by Si with the <Si1–O> bond length of 1.650 \AA , whereas the Si2 site has a site-occupancy factor (s.o.f.) of 0.10 with the <Si2–O> bond length equal to 1.87 \AA . The configuration around Si2 is remarkably similar to that observed in the $Ia\bar{3}d$ structure of katoite

**Fig. 3.** The relationship between the unit cell of nikkelnikovite (blue) and the ideal cubic unit cell of garnet (red).

(Sacerdoti and Passaglia 1985), where the Si site has the occupancy of 0.214 and the <Si–O> bond length is equal to 1.892 \AA .

'Hydrogarnet' substitution and short-range order in nikkelnikovite

It is usually implied that the 'hydrogarnet' substitution in garnets involves the substitution scheme $(\text{SiO}_4)^{4-} \leftrightarrow (\text{O}_4\text{H}_4)^{4-}$, where a silicate tetrahedron is replaced by a tetrahedral cluster of four $(\text{OH})^-$ groups (e.g. Geiger and Rossman 2018, 2020a,b and references therein). It is noteworthy that such a configuration-to-configuration scheme is favoured by the cubic symmetry of the $Ia\bar{3}d$ garnets, where all O atoms are symmetrically equivalent and Si is located in the 24d Wyckoff site with the point symmetry $\bar{4}$. The situation in nikkelnikovite is different, as the Si2 site has a trivial symmetry and its coordination environment is highly asymmetrical (Fig. 5). The O1, O2 and O3 sites are fully occupied and the occupancy of each site can be formulated as

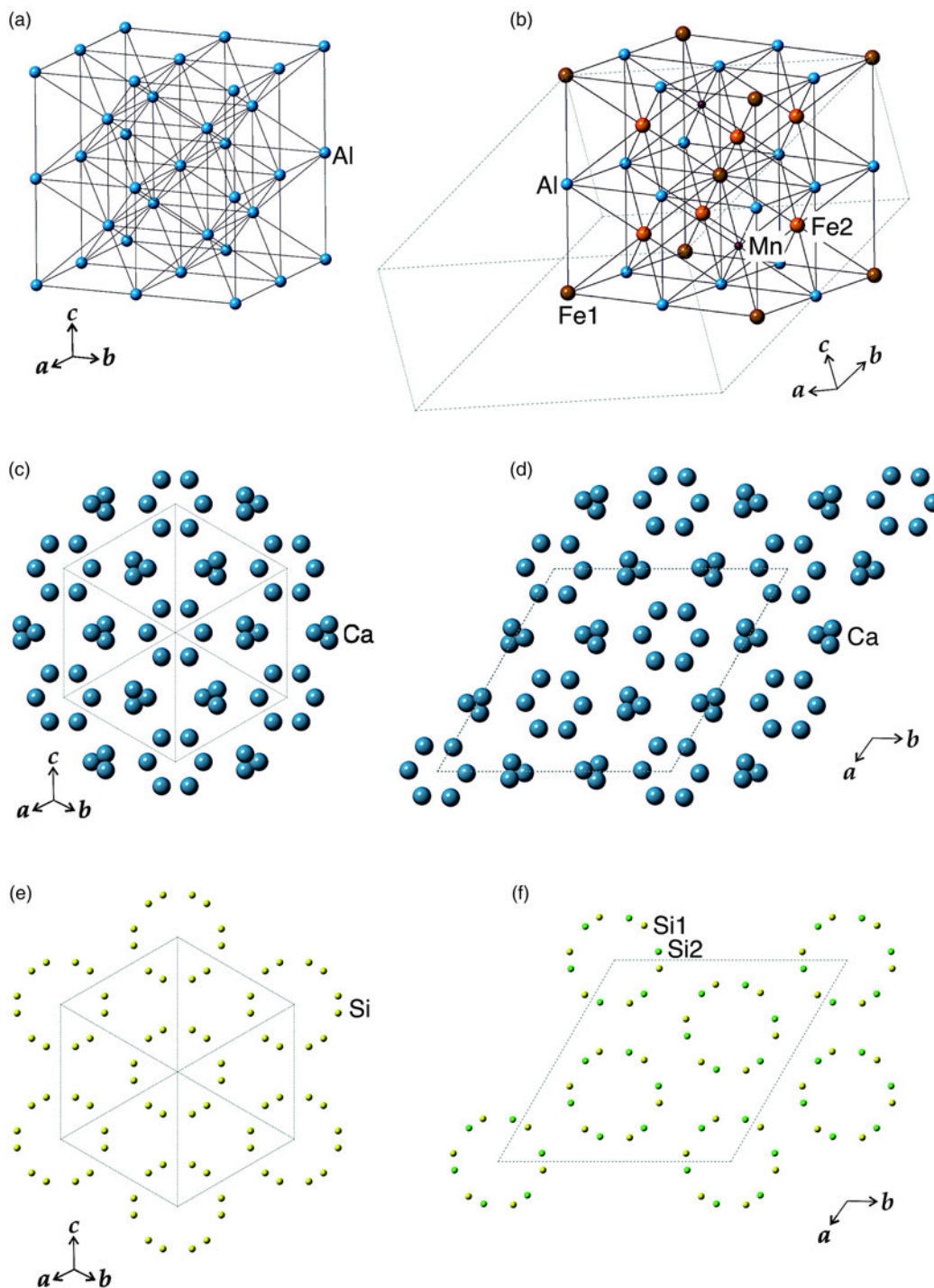
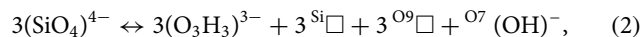


Fig. 4. The relationship between cation arrays in grossular (a, c, e) and nikkelnikovite (b, d, f): the arrays of octahedral cations (a, b), Ca (c, d) and Si sites (e, f).

(OH)_{0.882}O_{0.118}; i.e. if the Si2 site is vacant, these sites are populated by hydroxyl groups (in agreement with the 'hydrogarnet' substitution scheme). In contrast, the O9 site has a low occupancy and seems to be occupied only if the Si2 site is occupied by Si. This site has the neighbouring O7 site at 1.60 Å; i.e. the simultaneous occupation of the O9 and O7 sites by O is impossible. In contrast to the O9 site with trivial symmetry, the O7 site is located on the threefold axis and its assigned occupancy is (OH)_{0.882}. The substitution scheme for the O9 and O7 sites can therefore be

written as $3^{O9}O^{2-} \leftrightarrow ^{O7}(OH)^-$. The total 'hydrogarnet' substitution in nikkelnikovite corresponds to the scheme:



which results in the essential anion deficiency compared to the 'ideal' cubic garnets. For one formula unit, the substitution

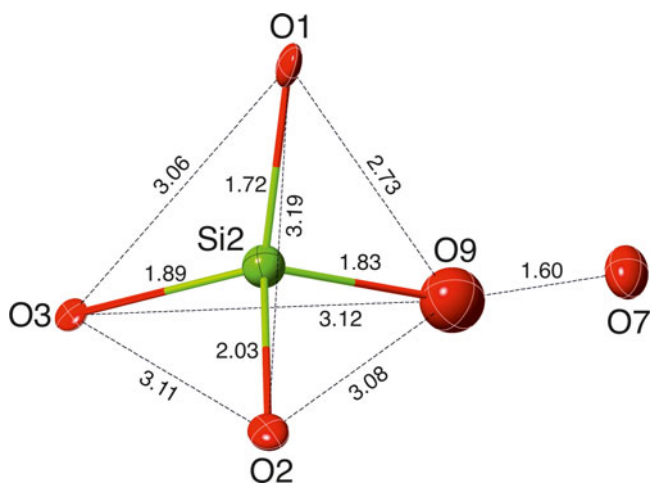
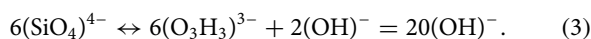
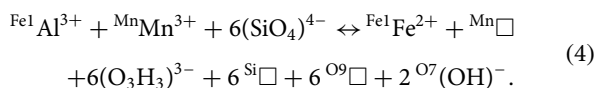


Fig. 5. The arrangement of anions around the Si2 site in nikmelnikovite.

scheme can be re-written as



This latter formulation agrees well with the empirical and idealised formulae of nikmelnikovite (see above; Krivovichev *et al.*, 2019). Note that both equations (2) and (3) are not charge-balanced. In the crystal of nikmelnikovite that we studied, the charge balance is achieved via two mechanisms: (1) incorporation of trivalent cations into the Mn site and (2) incorporation of Al^{3+} into the Fe1 site occupied primarily by Fe^{2+} . Thus, the total substitution scheme can be written as follows:



The $3^{\text{O}^9} \text{O}^{2-} \leftrightarrow \text{O}^7 (\text{OH})^-$ substitution mechanism affects the coordination environments of cations surrounding the respective configuration. In particular, the coordination of the Ca2 atom

changes from eightfold (the O9 site is occupied and the O7 site vacant) to sevenfold (the O7 site is occupied and the O9 site vacant). The same applies to the coordination of the Mn site, which seems to be occupied only if the O9 site is non-vacant. The other sites in nikmelnikovite are not affected by the ‘hydrogarnet’ substitution.

Discussion

Taking into account the results of this study, the crystal-chemical relations between the garnet archetype structure and the derivative nikmelnikovite structure can be described by the following series of imaginary modifications:

- (1) The symmetry is lowered according to the $Ia\bar{3}d \rightarrow R\bar{3}$ group-subgroup transition arising from the unit cell transformations defined by equation (1) above;
- (2) As a result, the cation sites are split according to the following sequences: $X \rightarrow \{X1, X2\}$; $Y \rightarrow \{Y1, Y2, Y3, Y4\}$; $Z \rightarrow \{Z1, Z2\}$;
- (3) the X sites remain occupied by Ca as, e.g. in grossular, andradite and katoite;
- (4) each Y site is occupied predominantly by a distinct chemical species: $Y1 \rightarrow \text{Al}$ (Al site), $Y2 \rightarrow \text{Fe}^{2+}$ (Fe1 site), $Y3 \rightarrow \text{Fe}^{3+}$ (Fe2 site) and $Y4 \rightarrow$ vacancy (Mn site);
- (5) one of the Z sites (Z1) remains occupied by Si, whereas the other site (Z2) is predominantly vacant; the modification of its coordination environment is described by equation (2) above.

The resulting structure of nikmelnikovite (Fig. 6) represents a porous three-dimensional octahedral–tetrahedral framework with cavities occupied by Ca^{2+} and H^+ cations. We note that further structural variations are possible in the garnet supergroup with the formation of various derivative octahedral–tetrahedral framework topologies.

The complete transformation from the ideal garnet structure $\{X_3\}[Y_2](Z_3)\phi_{12}$ to that of nikmelnikovite can be described as

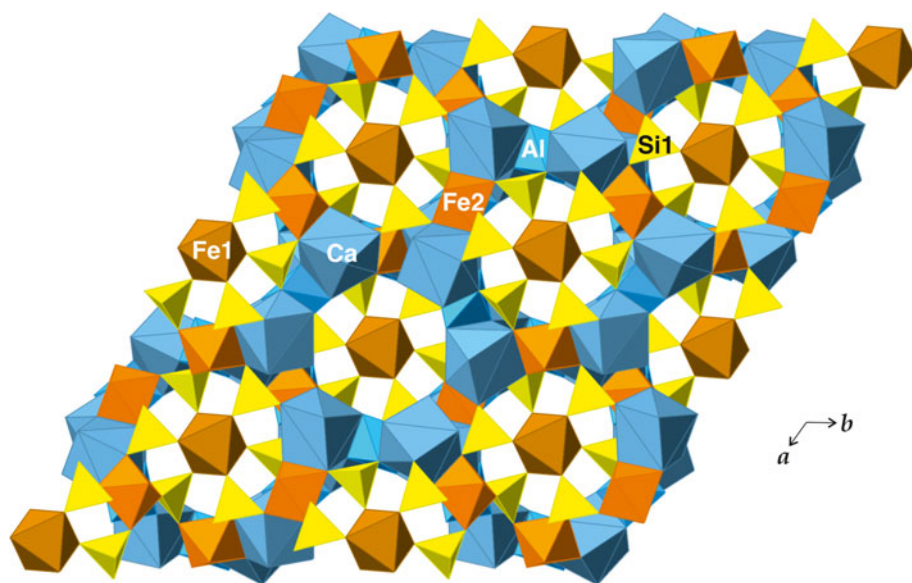
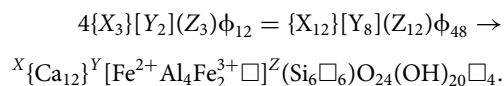


Fig. 6. The crystal structure of nikmelnikovite viewed along the c axis (only coordination polyhedra of cation sites with occupancies >50% are shown).

The latter formula takes into account the empirical Al:Fe ratio observed in nikhmelnikovite. The more strict end-member formula (Bosi *et al.*, 2019) should be written as $X\{Ca_{12}\}^Y[Fe^{2+}Al_3Fe_3^{3+}\square]^Z(Si_6\square_6)O_{24}(OH)_{20}\square_4$.

The crystal-chemical formula of nikhmelnikovite refined from the crystal structure can be written as $Ca_{12}(Al_{2.79}Fe_{0.21}^{3+})(Fe_{0.89}Al_{0.11})(Fe_{1.89}Al_{1.11})(\square_{0.882}Mn_{0.118})(SiO_4)_{6.708}(OH)_{17.64}$ or $Ca_{12}Al_{4.01}Fe_{2.10}^{3+}Fe_{0.89}Mn_{0.118}(SiO_4)_{6.708}(OH)_{17.64}$. This formula is in general good agreement with the empirical formula determined by the electron microprobe analysis reported by Krivovichev *et al.* (2019) (see Introduction).

The low symmetry of nikhmelnikovite that arises from complex substitutions and ordering phenomena is most likely the result of its low-temperature crystallisation. Nikhmelnikovite was precipitated on the surface of primary andradite crystals, probably by heterogeneous nucleation through epitaxy, as noted previously for H_4O_4 -substituted vesuvianite epitaxially grown on wiluite (Panikorovskii *et al.*, 2016). It is noteworthy that the structural complexity of nikhmelnikovite (4.529 bit/atom and 434.431 bit/cell, after H-correction: Krivovichev *et al.*, 2013, 2018) is higher than those of andradite, grossular (1.595 bit/atom and 127.637 bit/cell) and katoite (1.658 bit/atom and 192.315 bit/cell), which is the result of its lower symmetry and the greater number of structure sites. Such an increase in structural complexity is typical for low-temperature minerals formed after primary minerals with simpler structures.

It should be noted that low-symmetry birefringent garnets have been observed and studied previously (Shtukenberg *et al.*, 2005; Frank-Kamenetskaya *et al.*, 2007). A comprehensive review of the relevant literature was provided recently by Tančić *et al.* (2020). However, nikhmelnikovite is the first distinct garnet-supergroup member with a trigonal symmetry.

Acknowledgements. We are grateful to Evgeny Galuskin, Peter Leverett, and two anonymous referees for useful comments and Anton Chakhmouradian for correcting the English. This work was supported through the President of Russian Federation grant for young candidates of sciences (experimental work, grant MK-6240.2021.1.5 to T.L.P.) and Russian Science Foundation (theoretical analysis, grant 19-17-00038 to S.V.K.).

Supplementary material. To view supplementary material for this article, please visit <https://doi.org/10.1180/mgm.2021.55>

References

- Agilent Technologies (2014) *CrysAlis CCD and CrysAlis RED*. Oxford Diffraction Ltd, Yarnton, Oxfordshire.
- Armbruster T. and Geiger C.A. (1993) Andradite crystal chemistry, dynamic X-site disorder and structural strain in silicate garnets. *European Journal of Mineralogy*, **5**, 59–71.
- Bosi F., Hatert F., Hålenius U., Pasero M., Miyawaki R. and Mills S.J. (2019) On the application of the IMA-CNMNC dominant-valency rule to complex mineral compositions. *Mineralogical Magazine*, **83**, 627–632.

- Frank-Kamenetskaya O.V., Rozhdstvenskaya L.V., Shtukenberg A.G., Bannova I.I. and Skalkina Yu. A. (2007) Dissymmetrization of crystal structures of grossular-andradite garnets $Ca_3(Al,Fe)_2(SiO_4)_3$. *Structural Chemistry*, **18**, 493–503.
- Geiger C.A. and Armbruster T. (1997) $Mn_3Al_2Si_3O_{12}$ spessartine and $Ca_3Al_2Si_3O_{12}$ grossular garnet: structural dynamic and thermodynamic properties. *American Mineralogist*, **82**, 740–747.
- Geiger C.A. and Rossman G.R. (2018) IR spectroscopy and OH⁻ in silicate garnet: The long quest to document the hydrogarnet substitution. *American Mineralogist*, **103**, 384–393.
- Geiger C.A. and Rossman G.R. (2020a) Nano-size hydrogarnet clusters and proton ordering in calcium silicate garnet: Part I. The quest to understand the nature of “water” in garnet continues. *American Mineralogist*, **105**, 455–467.
- Geiger C.A. and Rossman G.R. (2020b) Micro- and nano-size hydrogarnet clusters in calcium silicate garnet: Part II. Mineralogical, petrological and geochemical aspects. *American Mineralogist*, **105**, 468–478.
- Grew E.S., Locock A.J., Mills S.J., Galuskin I.O., Galuskin E.V. and Hålenius U. (2013) Nomenclature of the garnet supergroup. *American Mineralogist*, **98**, 785–811
- Ivanyuk G.Yu., Yakovenchuk V.N. and Pakhomovsky Ya.A. (2002) *Kovdor*. Laplandia Minerals, Apatity, Russia. 320 pp.
- Krivovichev S.V. (2013) Structural complexity of minerals: information storage and processing in the mineral world. *Mineralogical Magazine*, **77**, 275–326.
- Krivovichev S.V., Krivovichev V.G. and Hazen R.M. (2018) Structural and chemical complexity of minerals: correlations and time evolution. *European Journal of Mineralogy*, **30**, 231–236.
- Krivovichev S.V., Yakovenchuk V.N., Panikorovskii T.L., Savchenko E.E., Pakhomovsky Ya.A., Mikhailova Yu. A., Selivanova E.A., Kadyrova G.I. and Ivanyuk G.Yu. (2019) Nikhmelnikovite, $Ca_{12}Fe^{2+}Fe^{3+}Al_3(SiO_4)_6(OH)_{20}$: a new mineral from the Kovdor massif (Kola Peninsula, Russia). *Doklady Earth Sciences*, **488**, 1200–1202.
- Lager G.A., Armbruster T., Rotella F.J. and Rossman G.R. (1989) OH substitution in garnets: X-ray and neutron diffraction, infrared, and geometric-modeling studies. *American Mineralogist*, **74**, 840–851.
- Moiseev M.M., Panikorovskii T.L., Aksenov S.M., Mazur A.S., Mikhailova J.A., Yakovenchuk V.N., Bazai A.V., Ivanyuk G.Y., Agakhanov A.A., Shilovskikh V.V., Pekov I.V., Kasatkin A.V., Rusakov V.S., Yapaskurt V.O., Karpenko V.Y. and Krivovichev S.V. (2020) Insights into crystal chemistry of the vesuvianite-group: manaevite-(Ce), a new mineral with complex mechanisms of its hydration. *Physics and Chemistry of Minerals*, **47**, 1–14.
- Panikorovskii T.L., Krivovichev S.V., Galuskin E.V., Shilovskikh V.V., Mazur A.S. and Bazai A.V. (2016) Si-deficient, OH-substituted, boron-bearing vesuvianite from Sakha-Yakutia, Russia: a combined single-crystal, ¹H MAS-NMR and IR spectroscopic study. *European Journal of Mineralogy*, **28**, 931–941.
- Sacerdoti M. and Passaglia E. (1985) The crystal structure of katoite and implications within the hydrogrossular group of minerals. *Bulletin de Mineralogie*, **108**, 1–8.
- Sheldrick G.M. (2008) A short history of SHELX. *Acta Crystallographica*, **A64**, 112–122.
- Shtukenberg A.G., Popov D.Yu. and Punin Yu.O. (2005) Growth ordering and anomalous birefringence in ugrandite garnets. *Mineralogical Magazine*, **69**, 537–550.
- Tančić P., Kremenović A. and Vulić, P. (2020) Structural dissymmetrization of optically anisotropic $Gr_{86\pm 1}Adr_{36\pm 1}Sp_{2}$ grandite from Meka Presedla (Kopaonik Mt., Serbia). *Powder Diffraction*, **35**, 7–16.